2022

Performance Analysis of a Novel Ejector-assisted Non-cascading Compression-absorption-resorption Refrigeration System

Anil Kumar

Anish Modi

Performance analysis of a novel ejector-assisted non-cascading compression-absorption-resorption refrigeration system

Anil KUMAR*, Anish MODI

Indian Institute of Technology Bombay, Department of Energy Science and Engineering,
Mumbai 400076, Maharashtra, India
Contact Information (anil.dese@iitb.ac.in)

* Corresponding Author

ABSTRACT

A refrigeration system utilizing heat to deliver cooling is among the best choices for process cooling and cold storage applications. The conventional absorption refrigeration system (ARS) is a heat driven refrigeration technology. However, the single-effect ARS has a low coefficient of performance (COP), whereas the double and triple effect systems operate at higher generator temperatures and are bulkier in size. This study proposes a novel ejector-assisted single-effect ammonia-water compression-absorption-resorption refrigeration system. An ejector is integrated to boost the absorber pressure and a compressor is used to increase the pressure of ammonia vapor at the desorber exit. The proposed single-effect system delivers two simultaneous refrigerating effects at −5 °C and 7 °C to the end-users without cascading. For a specific high pressure, the low pressure is varied in the feasible operating range, and a parametric analysis is performed to study the effect of the system compression ratio on the system performance (COP). The results indicate that at P_h = 14.5 bar, the proposed system attains a maximum COP of 0.98 at an absorber temperature of 40 °C and a generator temperature of 100 °C. In order to study the influence of the various operating parameters, the COP is calculated at the different absorber, desorber, and generator temperatures. The proposed system utilizes heat to deliver refrigerating effect at −5 °C, which saves electricity consumption by 36 % compared to a conventional vapor compression system.

1. INTRODUCTION

India's average temperature climbed by 0.7 °C between 1901 and 2018, and is anticipated to rise by 4.4 °C by the end of the twenty-first century (Singhal, Sharma, & Garg, 2021). It will have disastrous consequences for human health, agricultural production, and energy security. According to estimates, the number of cooling appliances would expand fourfold by 2050 compared to the present baseline of 3.6 billion (UNEP-IEA, 2020), and India will surpass the United States in cooling demand in 2024 with 38.8 million cooling appliance sales (Griffin et al., 2019). The existing cooling appliances are energy demanding and generally use vapour compression technology, with the mechanical compressor using around 80 % of the input energy (D.Coulomb, Dupont, & Pichard, 2015). Because of the use of power generated from fossil fuels and the usage of hazardous refrigerants, cooling has become the fastest rising source of green-house gas emissions. It is anticipated that the energy demand for thermal comfort in buildings will be about 6200 TWh energy in 2050, with the resulting green-house gas emissions warming the world by 0.5 °C by 2100 (Kalanki & Sachar, 2018). In this context, it is critical to design heat-driven cooling systems for increased performance and higher utilization of solar thermal energy or waste heat from industrial activities.

The absorption refrigeration system (ARS) is a well developed heat driven technology but limitations such as low coefficient of performance (COP), high initial cost, and system bulkiness limits its use despite the heat source availability. The COP can be further improved by multi-stage or multi-effect cycles which makes system even bulkier (Herold, Radermacher, & Klein, 2016). In order to reduce the system's bulkiness, researchers developed the absorption-resorption refrigeration system (ARRS) (Berdasco, Coronas, & Vallès, 2018). The ARRS is a modification of the ARS in which the condenser and evaporator are replaced with an absorber and a desorber, respectively. The ARRS features an extra degree of freedom over the ARS, allowing for greater design flexibility in terms of modulating the operating high and low pressures. The overall lower operational pressure values reduce component size and system bulkiness, however the COP decreases with decreasing operating pressure (Berdasco, Vallès, & Coronas, 2019). Kumar et al. (Kumar & Modi, 2022) suggested three versions of ejector-assisted ARRS in which an ejector was incorporated to enhance

absorber pressure. The authors found that the COP improves with increasing absorber pressure, and one of the proposed configuration attained a COP 15 % higher than the traditional ARRS. However, the COP drops with increasing absorber and resorber temperatures, limiting the applicability of the suggested system for applications requiring higher temperature lift.

There have been studies in which a mechanical compressor is integrated with an ARS to achieve the benefits of both vapour compression refrigeration system (VCRS) and ARS. Yari et al. (Yari, Zarin, & Mahmoudi, 2011) proposed hybrid generator-absorber-heat exchanger (GAX) ARS and compared the performance with the conventional GAX ARS. The authors observed that the second law efficiency is more sensitive to generator temperature compared to the COP. The second law efficiency was increased by 75 % whereas the COP was increased only by 5 % as the generator temperature changes from 400 K to 440 K. Cimsit et al. (Cimsit & Ozturk, 2012) studied a compression-absorption refrigeration cycle in which the condenser of the compression sub-cycle is cascaded to the evaporator of the absorption sub-cycle which reduces the temperature lift of the compression sub-cycle. In comparison to the conventional VCRS, the cascaded refrigeration cycle consumed 48-51 % less electricity. The proposed refrigeration cycle consumed 35 % less thermal energy with the lithium bromide-water working pair than the ammonia-water, resulting in a 33 % improvement in COP with lithium bromide-water over ammonia-water. Su et al. (Su & Zhang, 2017) proposed a compression-absorption refrigeration system coupled with a liquid desiccant dehumidification system. A compressor is integrated to compress the vapour generated from the generator and the condensation heat of the high pressure vapour is recovered and utilizes for the regeneration of liquid desiccant. The proposed system outperforms the conventional ARS by 34.97 %.

Farshi et al. (Farshi, Khalili, & Mosaffa, 2018) compared the performance of cascaded compression-absorption heat pump to compression, absorption, and hybrid heat pumps and observed the highest performance for the cascaded compression-absorption heat pump among the proposed heat pump configurations. Liu et al. (Liu, Ye, Bai, & He, 2019) investigated the performance of absorption-compression hybrid refrigeration systems using R1234yf/ionic liquid as the working pair and studied the effects of compressor position, compression ratio, and operating temperatures on the system COP. The authors observed that integrating the compressor reduces condenser heat load, and circulation ratio and the system achieved higher COP when the compressor is integrated between the absorber and evaporator than the compressor is integrated between the generator and condenser. Mohammadi et al. (Mohammadi, Khaledi, & Powell, 2019) proposed a hybrid dual-temperature absorption refrigeration system for refrigerating and freezing applications, and compared its performance to that of a dual-temperature CO_2 VCRS. The authors calculated the unit production cost of cooling (UPCC) to be USD 0.211/ton-hr for steam-driven system and USD 0.110/ton-hr for waste heat-drive system. Schweigler et al. (Schweigler, Helm, & Eckert, 2019) studied a flexible hybrid lithium bromide-water absorption-compression heat pump system for the increased temperature lift, reduced driving heat source temperature, and increased chilled water capacity. A turbo compressor was designed for the maximum pressure ratio of 3.5 and for the maximum revolutions of 90000 rpm. Yu et al. (Yu et al., 2019) conducted experimental investigation on a solar absorption-subcooled compression cooling system, in which the liquid refrigerant from the condenser outlet gets subcooled in the evaporator of a absorption sub-cycle. The proposed system achieved a maximum COP of 0.69 while delivering a cooling capacity of 4 kW.

Gao et al. (Gao, Xu, & Wang, 2021) proposed a hybrid absorption-compression heat pump in which a compression sub-cycle and an absorption sub-cycle are thermally coupled for a temperature lift of 90 °C. The system COP increased from 1.2 to 1.7 when the temperature lift was decreased from 110 °C to 70 °C. For the compression sub-cycle, the authors experimented with various refrigerants and found that R245fa, R152a, and R600 performed best. Parikhani et al. (Parikhani, Azariyan, Behrad, Ghaebi, & Jannatkhah, 2020) analysed a novel ammonia-water combined cooling, heating, and power cycle. The authors concluded that the efficiency of the system was improved with increasing evaporator temperature, ammonia mass fraction, and with decreasing separator pressure, generator temperature. Sioud et al. (Sioud, Bourouis, & Bellagi, 2019) investigated a double-effect absorption-recompression refrigeration cycle powered by an ejector. An ejector was installed in the external circuit to the absorption cycle, powered by the steam ranging from 240 °C to 340 °C. The authors observed a maximum COP of 1.57 for the proposed cycle which is 0.22 higher than the conventional double effect cycle. Kim et al. (Kim et al., 2013) performed an experimental study of operational characteristics of a compression-absorption high-temperature hybrid heat pump. The ammonia mass fraction was varied to determine the best operating conditions, and it was observed that for the ammonia mass fraction of 0.43, the system delivered hot water at 90 °C with maximum heating capacity of 10 kW . Pratihar et al. (Pratihar, Kaushik, & Agarwal, 2010) studied a 400 kW ammonia-water compression-absorption refrigeration system for the

chilled water application and the system performance was compared with a conventional vapour compression chiller with R22 as refrigerant. The influence of solution heat exchanger area on the COP, cooling capacity, and absorber heat duty was studied by the authors and concluded that increasing the solution heat exchanger area from 10 % to 30 % boosted the system COP by 16 %.

Reviewing the literature indicates that the compression-absorption-resorption refrigeration system without cascading has not been proposed and analysed until now. The objective of this study is to propose a novel configuration of the ejector-assisted compression-absorption-resorption refrigeration system (CARRS). The proposed configuration delivers two simultaneous refrigerating effects at 7 °C and −5 °C without cascading. The mathematical model of the proposed system is developed for the thermodynamic analysis (first and second law), and used to evaluate the performance of the proposed system. A detailed parametric study is carried out to investigate the influence of the operating parameters on the system performance. To emphasise the utilisation of heat (thermal energy), the electricity consumption by the proposed system is computed and compared with electricity consumption by a VCRS, for the same cooling capacity.

2. SYSTEM DESCRIPTION

The proposed CARRS is an extension of the ejector-assisted ARRS proposed by (Kumar & Modi, 2022), in which two compressors are incorporated between the desorber and absorber. Figure 1 shows the schematic diagram of the CARRS consisting of a generator, resorber, desorber, absorber, condenser, evaporator, splitter, two compressors, two pumps (SP), two throttle valves, two heat exchangers, and an ejector. The cycle uses ammonia-water mixture solution and operates at five pressure levels. The resorber and the generator operate at the highest pressure (P_{res} and P_{gen}), the absorber operates at compressor 2 or ejector 1 discharge pressure (P_{abs}), the condenser operates at the compressor 1 discharge pressure (P_{cond}), the evaporator operates at the saturation pressure corresponds to 7 °C (P_{evap}), and the desorber operates at the lowest pressure (P_{des}).

In the generator, the rich solution (-3-) receives desorption heat from the external heat source ($\dot{Q}_{gen}$) and boils the ammonia vapour. The generated ammonia vapour (-5-) enters into the resorber and gets absorbed by the lean solution (-14-). The remaining lean solution (-4-) passes through the heat exchanger 1 where it rejects heat to pre-heat the rich solution (-2-). The lean solution from heat exchanger 1 exit (-6-) enters into the ejector 1 as the primary flow. The resorber rejects the absorption heat ($\dot{Q}_{res}$) to the heat sink and the saturated solution from resorber exit (-8-) passes through the heat exchanger 2, where it gets subcooled by the lean solution stream (-13-). The subcooled solution (-9-) passes through the throttle valve 1 which reduces the solution pressure from P_{res} to P_{des}. The two-phase mixture from the throttle valve 1 (-10-) enters into the desorber. In the desorber, heat from the cooling load 1 generates ammonia vapour (-15-) which gets driven into the compressor 1 and the remaining lean solution (-11-) enters into the splitter, which divides stream (-11-) into two streams: (-12-) and (-16-). The stream (-12-) passes through the pump 2 which increases its pressure from P_{des} to P_{res}. The stream (-16-) goes into the ejector 1 as the secondary flow. The lean solution at P_{res} (-13-) receives heat of sub-cooling from the rich solution (-8-) while passing through the heat exchanger 2. The heated solution from the heat exchanger 2 (-14-) enters into the resorber where it absorbs the ammonia vapour from the generator (-5-). The primary nozzle of the ejector expands the primary flow (-6-) from P_{gen} to P_{des} and converts the pressure into the kinetic energy. Due to the pressure gradient, the secondary flow (-16-) gets driven into the ejector and mixes with the primary flow (-6-) in the mixing section. The mixed flow from the mixing section enters into the diffuser which converts the kinetic energy of the mixed flow into the pressure (P_{abs}) such that $P_{des} < P_{abs} < P_{gen}$.

The ammonia vapour from the desorber exit (-15-) goes into the compressor 1 which increases its pressure from P_{des} to the condenser pressure (P_{cond}). The compressed superheated vapour from the compressor 1 exit (-17-) enters into the condenser where it rejects the condensation heat ($\dot{Q}_{cond}$) to the heat sink. The saturated solution from the condenser passes through the throttle valve 2 which reduces the pressure from P_{cond} to the evaporator pressure (P_{evap}). The two-phase solution from the throttle valve 2 (-19-) enters into the evaporator where it receives heat from cooling load 2 and the generated ammonia vapour from evaporator (-20-) gets driven into the compressor 2. The compressor 2 compresses ammonia vapour from P_{evap} to P_{abs}. The compressed vapour from the compressor 2 gets absorbed by the lean solution from the ejector 1 exit (-7-) into the absorber, and this completes the cycle for the proposed CARRS.

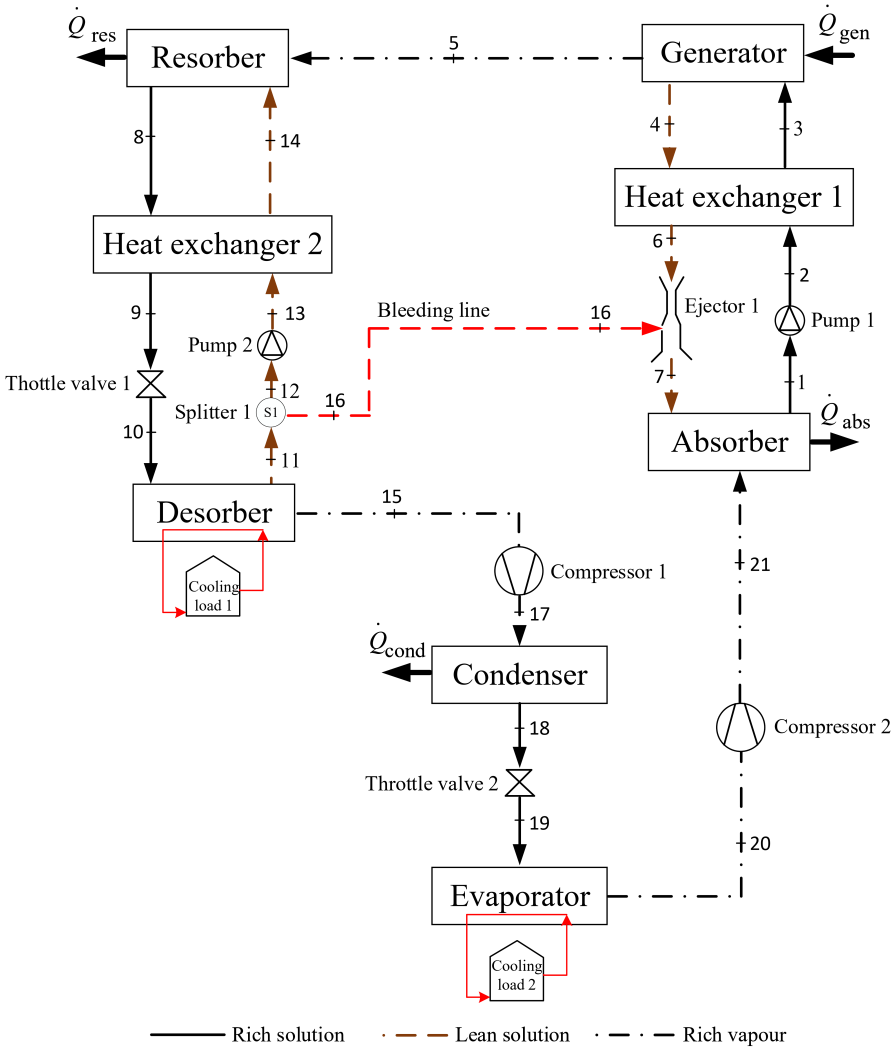

Figure 1: Schematic diagram of the ejector-assisted CARRS

3. SYSTEM SIMULATION AND ANALYSIS

A simulation model for the proposed CARRS is developed by considering each component as a control volume over which mass and energy balances are formulated. To evaluate the performance of the proposed CARRS, simulations are performed using Engineering Equation Solver (EES) software (Klein & Alvarado, 2021).

3.1 Ejector

In the proposed CARRS, an ejector is integrated at the absorber inlet to raise the absorber pressure. Figure 2 shows the schematic diagram of the ejector which recovers the expansion energy of the high pressure primary flow (-6-) and raise the pressure of the low pressure secondary flow (-16-) to P_{abs}. The integrated ejector is a liquid-liquid ejector in which and the modelling method based on the one-dimensional flow principle, proposed by (Chen, 1988) is adopted and the ejector is modelled as explained in Refs. (Farshi & Khalili, 2019; Kumar & Modi, 2022).

3.2 Thermodynamic analysis

To simulate the system, the principles of mass and energy balances are formulated for each component of CARRS considering as a control volume. It is assumed that the proposed system is a steady-state system operates at five pressure levels with negligible pressure drops in the piping and system components. The solution stream leaving the component is in the saturated state. The general equations for mass and energy balances over each component are as

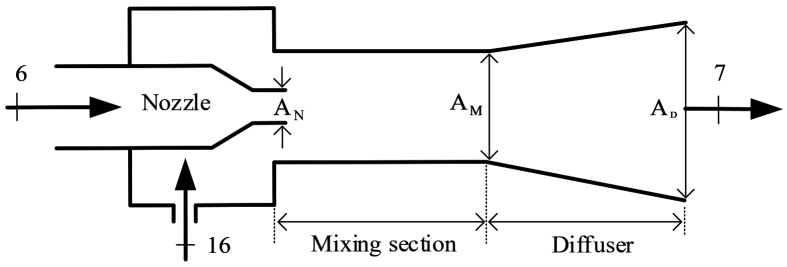

Figure 2: Schematic diagram of the ejector

follows:
Mass balance:

$$\sum \dot{m}_{\text{in}} = \sum \dot{m}_{\text{out}} \tag{1}$$

$$\sum \dot{m}_{\text{in}} \cdot x_{in} = \sum \dot{m}_{\text{out}} \cdot x_{\text{out}} \tag{2}$$

Energy balance:

$$\sum (\dot{m}_{\text{in}} \cdot h_{\text{in}}) - \sum (\dot{m}_{\text{out}} \cdot h_{\text{out}}) + \sum \dot{Q}_{\text{in}} - \sum \dot{Q}_{\text{out}} + \sum \dot{W}_{\text{in}} - \sum \dot{W}_{\text{out}} = 0 \tag{3}$$

In the above equations, $\dot{m}$ denotes mass flow rate, x denotes ammonia mass fraction, h denotes specific enthalpy, $\dot{Q}$ denotes rate of heat transfer, and $\dot{W}$ denotes rate of work transfer.
The coefficient of performance (COP) of the system:

$$\text{COP} = \frac{\dot{Q}_{\text{des}} + \dot{Q}_{\text{evap}}}{\dot{Q}_{\text{gen}} + \sum \dot{W}_{\text{pump}} + \sum \dot{W}_{\text{comp}}} \tag{4}$$

The generator flow ratio (f) is the ratio of the mass flow rate of ammonia rich solution entering into the generator to the mass flow rate of the ammonia vapour leaving the generator.

$$f = \frac{\dot{m}_{\text{s,in}}}{\dot{m}_{\text{v,out}}} = \frac{x_{\text{v,out}} - x_{\text{s,out}}}{\Delta x} \tag{5}$$

The savings in electricity consumption is:

$$\text{Savings} = \frac{\sum \dot{W}_{\text{comp,VCRS}} - \sum \dot{W}_{\text{comp,CARRS}}}{\sum \dot{W}_{\text{comp,VCRS}}} \tag{6}$$

3.3 Simulation method

To assess the performance of the proposed CARRS, the model has been developed using EES software and the properties of the ammonia-water mixture were estimated by using the relations developed by Ibrahim and Klein (Ibrahim, 1993). In order to consider the actual performance of the ejector, the efficiency of the ejector sections (nozzle, mixing section, and diffuser) are adopted from the Ref. (Farshi & Khalili, 2019) as shown in the Table 1. The ARRS provides an additional degree of freedom over the conventional ARS in terms of pressure modulation. For the constant operating temperature values, the highest operating pressure (P_{gen}) and the lowest operating pressure value (P_{des}) can be varied in the feasible range as explained in literature (Berdasco et al., 2019; Kumar & Modi, 2022). The feasible operating pressure range of P_{gen} and P_{des} is calculated for the input values given in Table 1, shown in the Figure 3. For a certain P_{gen}, P_{des} is considered as independent variable which is varied between $P_{\text{des,min}}$ and $P_{\text{des,max}}$ and the COP is calculated in relation to the compression ratio ($\frac{P_{\text{gen}}}{P_{\text{des}}}$). A detailed parametric study is performed to evaluate the influence of generator temperature, absorber temperature, and the condenser temperature on the system COP. In order to emphasis the benefits of the proposed CARRS, the electricity consumption by the both the compressors is computed and compared with the electricity consumption by the compressors in the VCRS having the same refrigerating capacity.

Table 1: Input data for the proposed configurations

T_{gen}	$T_{abs} = T_{res}$	T_{des}	T_{evap}	T_{cond}	ε_{HX}	η_N	η_M	η_D	η_{comp}
100 °C	40 °C	−5 °C	7 °C	40 °C	85 %	85 %	90 %	80 %	60 %

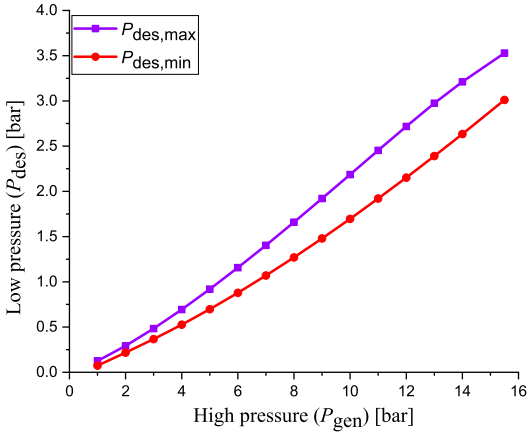

Figure 3: Feasible operating range of the absorption-resorption cycle

3.4 Model validation

The results from the numerical model of the absorption-resorption cycle are compared with the results obtained from two simulation and one experimental studies (Berdasco et al., 2019; Du, Yang, & Zhang, 1991; Jin et al., 2020). The comparison of the results and validation is presented by Kumar and Modi (Kumar & Modi, 2022). The results from the numerical model are found to be in good agreement with the references (Berdasco et al., 2019; Jin et al., 2020), with percentage deviation of less than 2.5 %.

4. RESULTS AND DISCUSSION

The aim of this research is to propose and assess the performance of a novel ejector-assisted CARRS. The proposed CARRS delivers two simultaneous refrigerating effects, out of which one may be used for cold storage and the other for process cooling at the same time. The simulations discussed above were performed for the input parameters listed in Table 1. A parametric study was also carried out to evaluate the system performance in terms of COP, as well as the influence of operating temperatures on the COP. In order to assess the advantages of the proposed configuration, the savings in terms of electricity consumption are computed.

4.1 Performance evaluation

Figure 4 compares the COP of the CARRS in relation to the system's compression ratio ($\frac{P_{gen}}{P_{des}}$) at P_{gen} = 14.5 bar, 13.5 bar, and 12.5 bar. At a given P_{gen} value, the P_{des} is varied between the $P_{des,max}$ and P_{min} in order to study the influence of $\frac{P_{gen}}{P_{des}}$ on COP. It may be observed that the COP increases to achieve the maximum value and then decreases with increasing the $\frac{P_{gen}}{P_{des}}$. For a given P_{gen} value, the P_{des} decreases with increasing the $\frac{P_{gen}}{P_{des}}$ resulting in lower operating pressures for the desrober and absorber. The cooling capacity of the system ($\dot{Q}_{des}$) and the generator flow ratio increases as the P_{des} decreases. With increasing the *f*, the consumption of heat into the generator ($\dot{Q}_{gen}$) increases. Therefore, COP increasing to a maximum value and then decreases with increasing the $\frac{P_{gen}}{P_{des}}$. It may also be observed that, for a given $\frac{P_{gen}}{P_{des}}$, the COP decreases with decreasing the P_{gen} and a maximum COP of 0.98 is observed for P_{gen} = 14.5 bar. This is because, with decreasing the P_{gen}, P_{des} decreases, as shown in Figure 3 resulting in lower operating pressure for the absorber. For the constant operating temperature, the ammonia mass fraction of solution leaving the absorber decreases with decreasing the absorber pressure causing higher generator flow ratios. Due to this, the heat consumption

for the desorption process into the generator increases with decreasing the P_{gen}, as shown in Figure 5.

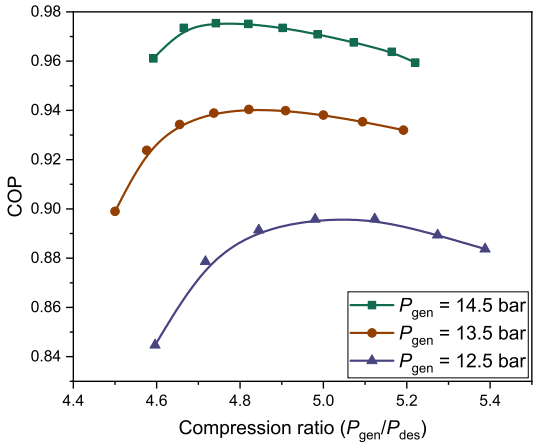

Figure 4: Variation of COP with compression ratios at different P_{gen} values

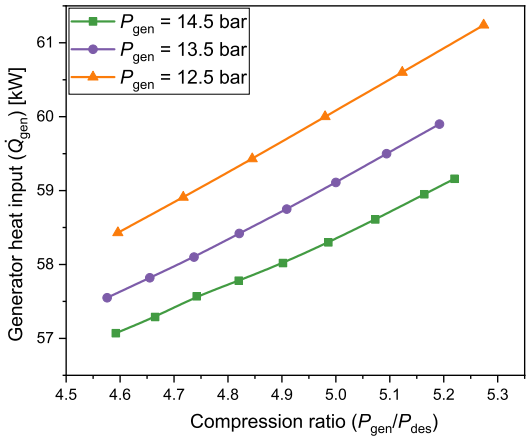

Figure 5: Variation of generator heat input with compression ratios at different P_{gen} values

4.2 Influence of generator temperature

Figure 6 shows the influence of generator temperature on the COP in relation to the desorber temperatures. It may be observed that the COP increases to gain the maximum value and then decreases with increasing the generator temperature. At a given P_{gen}, the generator flow ratio decreases with increasing the generator temperature as a result the heat consumption by the generator decreases. But, for a given pressure, the water holding capacity of ammonia increases as the temperature increases and heat requirement for the desorption of ammonia from the water increases. Thus, the COP increases to attain a maximum value and then decreases with increasing the generator temperature.

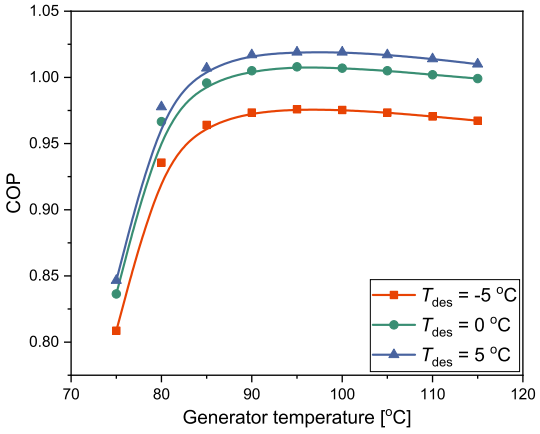

Figure 6: Influence of generator temperature on the COP in relation to the desorber temperatures

4.3 Influence of condenser temperature

Figure 7 shows the influence of condenser temperature to the COP in relation to the compression ratio at P_{gen} = 14.5 bar. It may be observed the COP increases to attain the maximum value and than decreases with increasing the compression ratio, as explained in the section 4.1. It may also be observed that for a given compression ratio, the COP increases

with decreasing the condenser temperature and a maximum COP of 1.01 is observed at a condenser temperature of 35 °C. This is because with decreasing the condenser temperature, the temperature lift and the compression ratio for the compressor 1 decreases. As a result, the electricity consumption by the compressor 1 decreases and the COP increases.

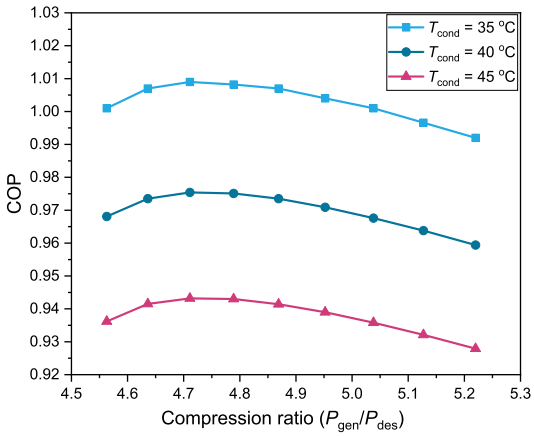

Figure 7: Influence of condenser temperature to the COP

4.4 Electricity savings

Figure 8 shows the comparison of the savings in electricity consumption at P_{gen} = 14.5 bar, 13.5 bar, and 12.5 bar in relation to the compression ratio. It may be observed that the savings in electricity consumption decreases with decreasing the P_{gen} and the maximum savings of 36 % is achieved at P_{gen} = 14.5. The operating pressure for the desorber decreases with decreasing the P_{gen}, as shown in Figure 2. Due to this, the temperature lift or compression ratio for the compressor 1 increases resulting in higher electricity consumption by the compressor 1. Thus, the savings decreases with decreasing the P_{gen}.

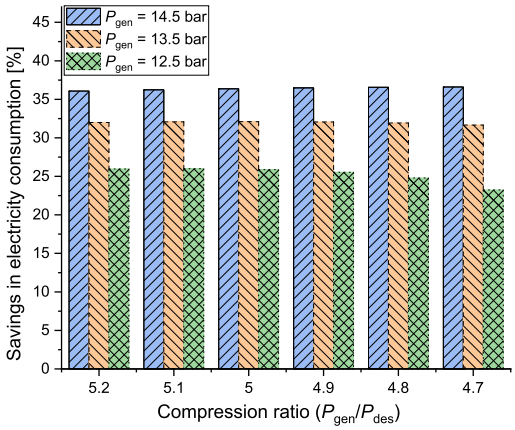

Figure 8: Savings in electricity consumption at different P_{gen} values

4.5 Discussion

The proposed CARRS has the following advantages over the conventional hybrid cascaded ARS and the double effect ammonia-water ARS: (a) delivers two simultaneous refrigerating effects at two different temperatures, and (b) attains a

maximum COP of 0.98 at the generator temperature of 100 °C. Also, compared to a VCRS the proposed system utilises thermal energy from the industrial process heat or renewable to deliver refrigerating effect at −5 °C, which saves the electricity consumption by 36 %. The future research may focus to optimize the CARRS for the maximum utilization of waste heat and minimum electricity consumption.

5. CONCLUSIONS

The refrigeration system which utilizes waste heat for cold generation is among the best choices for air conditioning, and cold storage. In this study, a novel ejector-assisted CARRS is proposed to utilise the waste heat. The proposed CARRS delivers two refrigerating effects simultaneously, out of which one may be used for cold storage when thermal energy is available. At the same time, others may be used for the air conditioning as per the requirement. The COP of the system increases with increasing the compression ratio and attains a maximum COP of 0.98 for P_{gen} = 14.5 bar. The COP increases with increasing the desorber temperature, and for the desorber temperature of 5 °C, the system achieves a maximum of COP of 1.03 at a generator temperature of 100 °C. It was observed that the electricity consumption increases with increasing the condenser temperature and with decreasing the P_{gen} values. The proposed CARRS saves electricity consumption by 36 % with compared to a conventional VCRS, highlighting the utilization of thermal energy (heat).

NOMENCLATURE

COP	coefficient of performance	(-)
h	specific enthalpy	(kJ/kg)
$\dot{m}$	mass flow rate	(kg/s)
P	pressure	(bar)
$\dot{Q}$	rate of heat transfer	(kW)
T	temperature	(°C)
$\dot{W}$	rate of work transfer	(kW)
ε	effectiveness	(-)
η	efficiency	(-)
Subscript		
cond	condenser	
comp	compressor	
des	desorber	
D	diffuser	
evap	evaporator	
gen	generator	
HX	heat exchanger	
N	nozzle	
M	mixing section	
res	resorber	

REFERENCES

Berdasco, M., Coronas, A., & Vallès, M. (2018). Study of the adiabatic absorption process in polymeric hollow fiber membranes for ammonia/water absorption refrigeration systems. *Applied Thermal Engineering*, *137*, 594–607.

Berdasco, M., Vallès, M., & Coronas, A. (2019). Thermodynamic analysis of an ammonia/water absorption–resorption refrigeration system. *International Journal of Refrigeration*, *103*, 51–60.

Chen, L.-T. (1988). A new ejector-absorber cycle to improve the cop of an absorption refrigeration system. *Applied Energy*, *30*(1), 37–51.

Cimsit, C., & Ozturk, I. T. (2012). Analysis of compression–absorption cascade refrigeration cycles. *Applied Thermal Engineering*, *40*, 311–317.

D.Coulomb, Dupont, J., & Pichard, A. (2015). 29th informatory note on refrigeration technologies. *The Role of Refrigeration in the Global Economy*.

Du, K., Yang, S., & Zhang, S. (1991). Experimental analysis and research of an aqua ammonia absorption-resorption

heat pump. *J Eng Thermophys*, *3*(12), 229–233.
Farshi, L. G., & Khalili, S. (2019). Thermoeconomic analysis of a new ejector boosted hybrid heat pump (ebhp) and comparison with three conventional types of heat pumps. *Energy*, *170*, 619–635.
Farshi, L. G., Khalili, S., & Mosaffa, A. (2018). Thermodynamic analysis of a cascaded compression–absorption heat pump and comparison with three classes of conventional heat pumps for the waste heat recovery. *Applied Thermal Engineering*, *128*, 282–296.
Gao, J., Xu, Z., & Wang, R. (2021). An air-source hybrid absorption-compression heat pump with large temperature lift. *Applied Energy*, *291*, 116810.
Griffin, C., Fisher, D., Haider, S., Labalme, E., Saini, D., Constantino, S., … Owen, G. (2019). The cooling imperative. forecasting the size and source of future cooling demand. *www.eiu.com/graphics/marketing/pdf/TheCoolingImperative2019.pdf* .
Herold, K., Radermacher, R., & Klein, S. (2016). *Absorption chillers and heat pumps, second edition*. CRC press.
Ibrahim, O. (1993). Thermodynamic properties of ammonia-water mixtures. In *Ashrae transactions: Symposia* (Vol. 93, p. 1495).
Jin, Z., Li, S., Xu, M., Xu, C., Feng, L., & Du, K. (2020). The effect of lithium bromide on the performance of ammonia-water absorption-resorption heat pump system. *Applied Thermal Engineering*, *181*, 115888.
Kalanki, A., & Sachar, S. (2018). Revolutionizing the air conditioner industry to solve the cooling challenge. *https://globalcoolingprize.org/solving-the-global-cooling-challenge/, Online accessed on 22/12/2021*.
Kim, J., Park, S.-R., Baik, Y.-J., Chang, K.-C., Ra, H.-S., Kim, M., & Kim, Y. (2013). Experimental study of operating characteristics of compression/absorption high-temperature hybrid heat pump using waste heat. *Renewable Energy*, *54*, 13–19.
Klein, S., & Alvarado, F. (2021). EES: engineering equation solver for the microsoft windows operating system, v11.145-3d. *F-Chart Software*.
Kumar, A., & Modi, A. (2022). Thermodynamic analysis of novel ejector-assisted vapour absorption-resorption refrigeration systems. *Energy*, 123154.
Liu, X., Ye, Z., Bai, L., & He, M. (2019). Performance comparison of two absorption-compression hybrid refrigeration systems using r1234yf/ionic liquid as working pair. *Energy Conversion and Management*, *181*, 319–330.
Mohammadi, K., Khaledi, M. S. E., & Powell, K. (2019). A novel hybrid dual-temperature absorption refrigeration system: Thermodynamic, economic, and environmental analysis. *Journal of cleaner production*, *233*, 1075–1087.
Parikhani, T., Azariyan, H., Behrad, R., Ghaebi, H., & Jannatkhah, J. (2020). Thermodynamic and thermoeconomic analysis of a novel ammonia-water mixture combined cooling, heating, and power (cchp) cycle. *Renewable Energy*, *145*, 1158–1175.
Pratihar, A., Kaushik, S., & Agarwal, R. (2010). Simulation of an ammonia–water compression–absorption refrigeration system for water chilling application. *International Journal of refrigeration*, *33*(7), 1386–1394.
Schweigler, C., Helm, M., & Eckert, T. (2019). Flexible heat pump or chiller with hybrid water/libr absorption/compression cycle. *International Journal of Refrigeration*, *105*, 178–187.
Singhal, A., Sharma, S., & Garg, T. (2021). Transitioning to super energy-efficient room air conditioners: forstering icap implementation. *New Delhi: Alliance for an Energy Efficient Economy (AEEE)*.
Sioud, D., Bourouis, M., & Bellagi, A. (2019). Investigation of an ejector powered double-effect absorption/recompression refrigeration cycle. *International Journal of Refrigeration*, *99*, 453–468.
Su, W., & Zhang, X. (2017). Thermodynamic analysis of a compression-absorption refrigeration air-conditioning system coupled with liquid desiccant dehumidification. *Applied Thermal Engineering*, *115*, 575–585.
UNEP-IEA. (2020). Cooling emissions and policy synthesis report. *https://www.unep.org/resources/report/cooling-emissions-and-policy-synthesis-report*.
Yari, M., Zarin, A., & Mahmoudi, S. (2011). Energy and exergy analyses of gax and gax hybrid absorption refrigeration cycles. *Renewable energy*, *36*(7).
Yu, J., Li, Z., Chen, E., Xu, Y., Chen, H., & Wang, L. (2019). Experimental assessment of solar absorption-subcooled compression hybrid cooling system. *Solar Energy*, *185*, 245–254.

ACKNOWLEDGMENT

The authors gratefully acknowledge the financial support from the Ministry of Education, Government of India under the PMRF scheme.